

# Distributed insulation monitoring for U.K. 650-V railway signaling power supplies using rectified current difference pattern tracking

Xu, Guangqiao; Weston, Paul; Hillmansen, Stuart

DOI:

[10.1109/TTE.2018.2826441](https://doi.org/10.1109/TTE.2018.2826441)

License:

Other (please specify with Rights Statement)

Document Version

Peer reviewed version

Citation for published version (Harvard):

Xu, G, Weston, P & Hillmansen, S 2018, 'Distributed insulation monitoring for U.K. 650-V railway signaling power supplies using rectified current difference pattern tracking', *IEEE Transactions on Transportation Electrification*, vol. 4, no. 2, pp. 605-615. <https://doi.org/10.1109/TTE.2018.2826441>

[Link to publication on Research at Birmingham portal](#)

## Publisher Rights Statement:

Checked for eligibility: 12/09/2018

© 2018 IEEE. Personal use of this material is permitted. Permission from IEEE must be obtained for all other uses, in any current or future media, including reprinting/republishing this material for advertising or promotional purposes, creating new collective works, for resale or redistribution to servers or lists, or reuse of any copyrighted component of this work in other works.

G. Xu, P. Weston and S. Hillmansen, "Distributed Insulation Monitoring for U.K. 650-V Railway Signaling Power Supplies Using Rectified Current Difference Pattern Tracking," in *IEEE Transactions on Transportation Electrification*, vol. 4, no. 2, pp. 605-615, June 2018.  
doi: 10.1109/TTE.2018.2826441

## General rights

Unless a licence is specified above, all rights (including copyright and moral rights) in this document are retained by the authors and/or the copyright holders. The express permission of the copyright holder must be obtained for any use of this material other than for purposes permitted by law.

- Users may freely distribute the URL that is used to identify this publication.
- Users may download and/or print one copy of the publication from the University of Birmingham research portal for the purpose of private study or non-commercial research.
- User may use extracts from the document in line with the concept of 'fair dealing' under the Copyright, Designs and Patents Act 1988 (?)
- Users may not further distribute the material nor use it for the purposes of commercial gain.

Where a licence is displayed above, please note the terms and conditions of the licence govern your use of this document.

When citing, please reference the published version.

## Take down policy

While the University of Birmingham exercises care and attention in making items available there are rare occasions when an item has been uploaded in error or has been deemed to be commercially or otherwise sensitive.

If you believe that this is the case for this document, please contact [UBIRA@lists.bham.ac.uk](mailto:UBIRA@lists.bham.ac.uk) providing details and we will remove access to the work immediately and investigate.

Guangqiao Xu (University of Birmingham),  
Paul Weston (University of Birmingham)  
Stuart Hillmansen (University of Birmingham)

Corresponding Author: Name: Mr. Guangqiao Xu  
Email: [GXX256@bham.ac.uk](mailto:GXX256@bham.ac.uk)  
Contact No. : +447521505638  
Address: Dept, Electronic, Electrical and System Engineering, University Of  
Birmingham, Edgbaston, Birmingham, B15 2TT, United Kingdom.

Word, Windows 10

### Abstract

Signalling power is crucial to an operational railway system as any signalling power failure results in serious operational and financial impacts. Therefore, intelligent condition monitoring and accurate fault location are important for the railway industry. This paper introduces a novel distributed insulation monitoring method for railway signalling power system that can monitor continually the resistive earth leakage current and determine the location of the leakage point by tracking the rectified current difference pattern. This method can be used for extended signalling power distribution networks with multiple branches and requires no external power supply or signal injection.

**Key Words-** Insulation Failure, Cross-correlation, Leakage Current, Fault Location

### 1. Introduction

UK railway operators unavoidably suffer from a variety of faults in signalling power supply system owing to various reasons such as improper cable laying, faulty connections, thermal breakdown, electrical breakdown, and insulation failure. The inability to identify those faults in a timely manner may cause a sudden loss of power to critical signalling equipment (e.g. signalling lamps, point machines) which will eventually incur a financial impact due to high maintenance costs, poor performance and punctuality penalty payments [1]. Repairing faults can be rather costly in terms of manpower and time. Therefore, an intelligent signalling power monitoring system with robust and accurate fault locating techniques are rather important to the railway industry.

650 V railway signalling power supply system, typically an IT network, is designed so that it can provide continue to supply power during an insulation fault without having the risk of an indirect contact hazard. However, the first earth fault needs to be located as soon as possible as a second fault will leave the connected equipment in a hazardous state, and sensitive loads will operate at possible under/over voltage in the presence of the first fault. Under a healthy condition, the insulation resistance of the power cable will be around 8-12 MΩ/km with its capacitance to earth evenly distributed at approximately 0.2-0.3 μF [2].

### 2. Existing Earth Fault Locating Methods and Insulation Monitoring

In a LV IT distribution network, the most common insulation monitoring techniques are those with active insulation resistance measurement by creating a leakage path via a known high resistance grounding so that leakage current can be measured and leakage resistance can be calculated. Given that the leakage current has both capacitive and resistive components, phase locked demodulation is usually required to extract the resistive component. In addition, by measuring the insulation resistance only, accurate distance to fault calculation is not possible, which is why tracer-based earth fault locating techniques are used after an earth fault is detected. High frequency signals are injected into the faulty cable and technical operators are required to search along the cable with designated portable devices that can find where the induced signal disappears. The maximum search distance depends on the signal attenuation as well as the level of complexity of system configuration. Tracking down an earth fault using a portable clamp is a time-consuming activity.

Various cable diagnostic techniques are currently in use and can be generally categorised by their fundamental principles: a) Impedance-based terminal methods [3-12]. b) Wavelet analysis-based methods [13-19]. c) Thumper and Tracer based methods [2, 20]. Due to their relative simplicity, impedance-based methods are frequently used to detect and locate cable faults. Time domain reflectometry, one of the most commonly used methods in this discipline, has been at the forefront of cable testing for decades, however, like most other

terminal methods, it requires a rather low fault resistance for it to work correctly [2]. Very low frequency AC injection is sometimes used in very long IT networks [5]. It can extract the resistive component of the leakage current that flows through insulation impedance by computing the phase shift after demodulation. ARM (Arc reflection method) based methods, ICE (impulse current equipment) and bridge methods have their advantages in locating high resistance faults but require loads to be disconnected from the feeder. Travelling-based methods mostly rely on measuring and extracting transient voltage and currents that are caused by a system abnormality. By identifying and comparing the arrival instance of fault waves from one or more measuring points, the location of the fault can be estimated. Tracer-based methods are in general more reliable and accurate but rather time-consuming, thus it is used when other approaches fail [21].

Several hybrid reflectometry techniques were introduced to locate small defects in a cable recently. Research in [22] injects pseudo random binary sequence into the cable instead of a step signal. By cross correlating the reflection with the injected signal, it substantially increases the signal-to-noise ratio so that small reflections can be revealed while noises and random disturbances get filtered out. Similar correlation principles are also used in other hybrid reflectometry technologies to overcome the poor signal noise ratio issue. Joint time frequency domain reflectometry introduced in research [23] successfully detected small cable defects during the accelerated thermal aging test and both research [24] and [25] showed that it is also possible to located intermittent cable faults using spread spectrum time domain reflectometry.

However, it is impractical to apply hybrid reflectometry-based technologies for railway signaling power monitoring for several reasons. Firstly, unlike aircraft cables, typically there are several feeders off the same isolation transformer and each feeder runs between 5 to 15km with some at up to 20 km. High frequency testing like SSTDR (Spread Spectrum Time Domain Reflectometry) comes with inevitable severe signal attenuation, because railway signaling power cables are not designed to carry high frequency signals. Since the injected signal will normally disappear long before it reaches the end of the cable, it is mandatory to have a distributed signal injection arrangement in order to cover the whole length of the feeding cable. Secondly, despite of the high cost of installation and maintenance, reflectometry-based technologies are very sensitive to internal interferences. For instance, multiple branches will produce multiple reflections from cable joints and even single branch will have multiple reflections from each function supply point. Considering that railway signaling power supply will normally have dozens of function supply points, in order to differentiate fault reflections from other reflections, sophisticated pre-calibration process must be done before the fault location process. With a known system configuration, the signal propagation velocity can be estimated, after which the distance to fault calculation can be done accordingly. However, the difficulty of distinguishing fault reflections from others will increase exponentially as the number of FSP (Function Supply Point) and branches increase. Last but not least, each signalling power supply configuration will be different across the whole railway network. Non-repetitive calibration work is rather time consuming because each system is different across the whole network. In addition, re-calibration is also required when circumstances change, for example, new equipment gets added to the network or a faulty equipment gets temporary disconnected for maintenance.

This paper introduces an alternative insulation monitoring and fault location method for the 650 V railway signalling power distribution system that utilizes the source signal itself instead of injected ones.

### 3. Method Explanation

Figure 1 shows a simplified circuit arrangement for the proposed earth fault locating method for a 650 V signalling power supply.

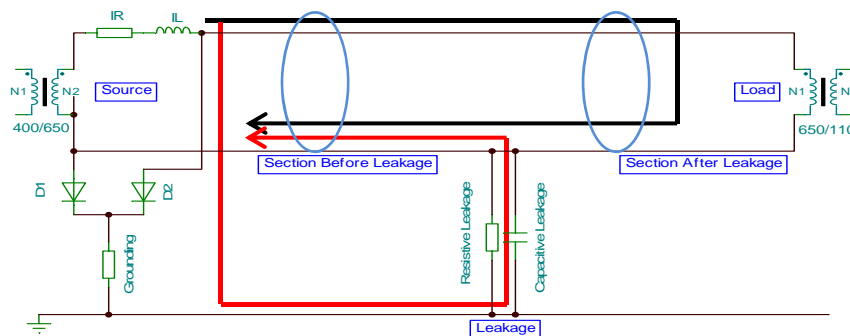


**Figure 1 Simplified System Arrangement**

At the transformer side of the feeder, a potentially adjustable, high resistance grounding system is set up for both active conductors so that it creates a low current path for earth leakage currents to flow through. Two 1 kv rated diodes are used here to force any earth leakage current to flow in one direction only. In the event of leakage from either cable core to earth, this arrangement creates an unequal outgoing and returning currents in the cable.

### 3.1. Fault Identification

Rectifying the leakage current makes it possible to measure the resistive leakage only. The insulation conditions of the two conductors in the cable can be determined individually by measuring the voltage across the grounding resistor ( $V_R$ ) without any demodulation to extract the resistive components. The insulation condition will be considered healthy as long as the measured leakage current is below pre-set thresholds. Figure 2 shows a simulation of normal operation. The small and narrow peaks are caused by the diodes leaking a small current at low forward voltages. The first peak in currents is due to the capacitance charging of the cable.

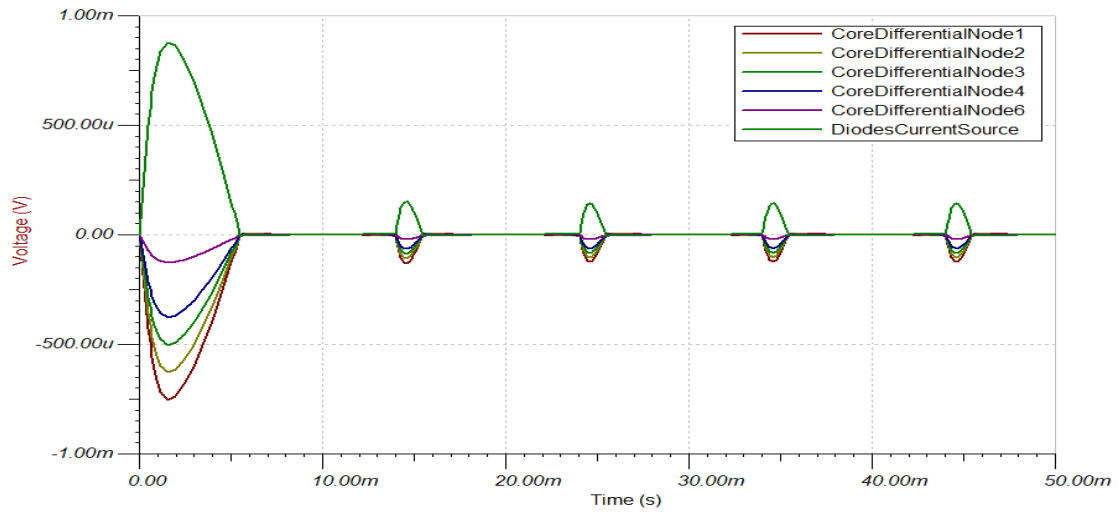


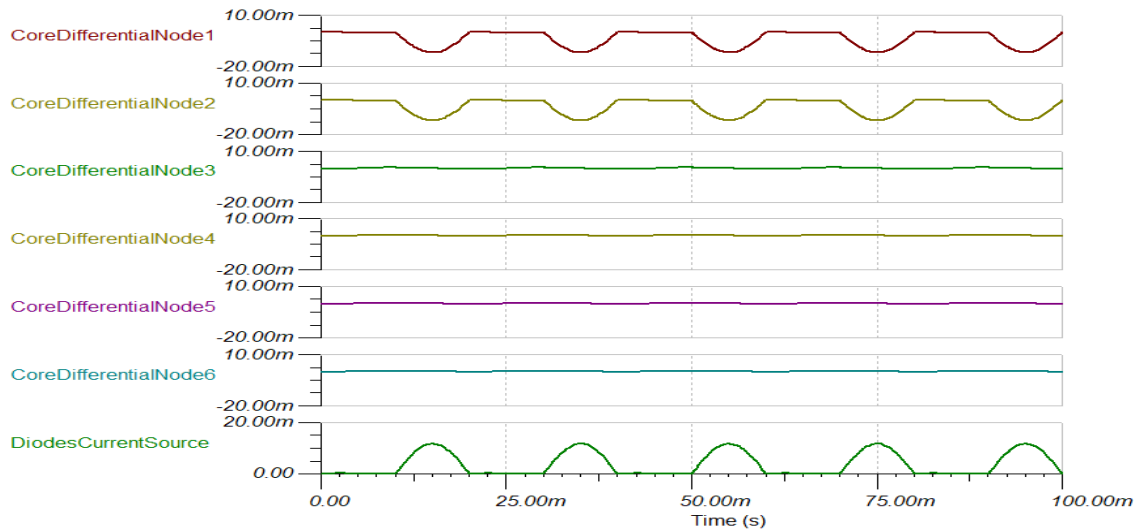
**Figure 2 Insulation Condition Normal**

### 3.2. Fault Locating

The differences ( $I_D$ ) between the outgoing ( $I_O$ ) and returning ( $I_R$ ) current within the cable can be used to determine the location of the fault. As the rectified current difference ( $I_D$ ) will only travel through the cable section prior to the location of the earth fault, it is possible to locate the fault by analysing current differences from a monitoring system deployed in a distributed fashion along the feeder.

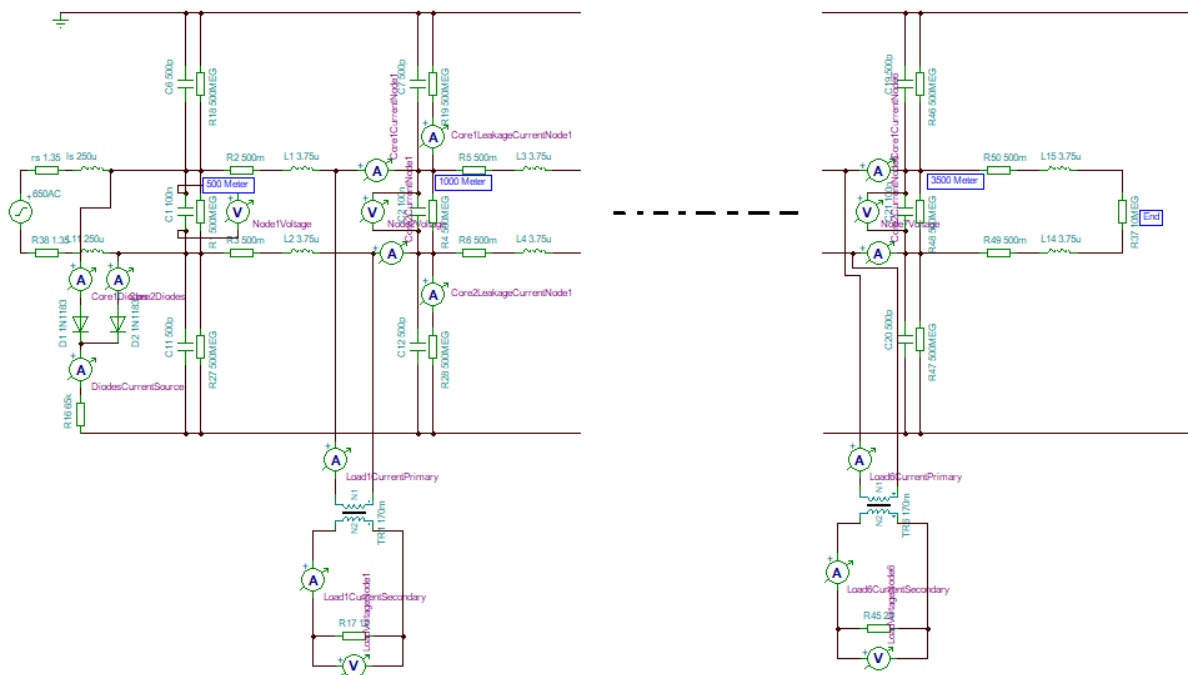
The out ( $I_O$ ) and return ( $I_R$ ) currents differ by only a tiny amount compared to the load current, making observation of the difference difficult. Any current difference ( $I_D$ ) before the location of the fault will have a distinctive waveform compared to those picked up after the fault location. Monitoring the voltage across the grounding resistor ( $V_R$ ) (or resistors) reveals the insulation condition of the whole cable, whereas the current difference patterns from the distributed current sensors can further determine whether the cause is distributed earth leakage or leakage from one particular section (as shown in Figure 3).

Very accurate measurement or complicated sensor calibration is not required in this case, since it is the general magnitude of a particular pattern that matters rather than the exact value itself. Even in the case of high leakage resistance, which will have very small earth leakage current, the periodic signal can still be extracted by phase-locked-loop techniques. The smaller the fault, the longer the correlation time that will be needed; therefore, fixed installation with selective data collection is preferable. In addition, the grounding resistor at the source end can be varied to control the signal to noise ratio.



## 4. Simulation

A T-section transmission line model was used for the signalling power cable with all the electrical parameters obtained for a 100 m 35 mm<sup>2</sup> aluminium B2 cable. Figure 4 shows a 650 V AC signalling power model with different types of signalling equipment powered off 650/110 stepdown transformers.



#### 4.1. Cable Deterioration

Excessive leakage current does not always mean an earth fault at an isolated location. Sometimes an aged cable that has been in service for over a decade can have poor insulation evenly across the whole cable, providing a

relatively higher total leakage current without any dominant single location earth fault present. As shown in Figure 5, the grounding resistor reading shows both conductors have observable earth leakage current, whereas the current difference ( $I_D$ ) indicates it is leaking from all over the cable rather than from a single earth fault. The same principle applies to very large system configurations. Therefore, different system arrangements should have different set-values for insulation monitoring.

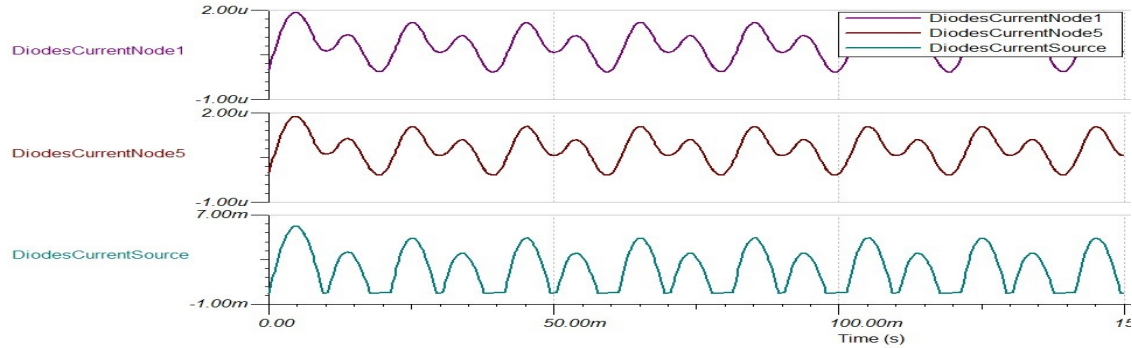


**Figure 5 Simulation results.**

#### 4.2. Single Earth Fault

As explained above, the rectified current difference pattern will move along with the location of the earth fault. Thus, if it is a single earth fault situation, the fault can be located where the rectified signal disappears.

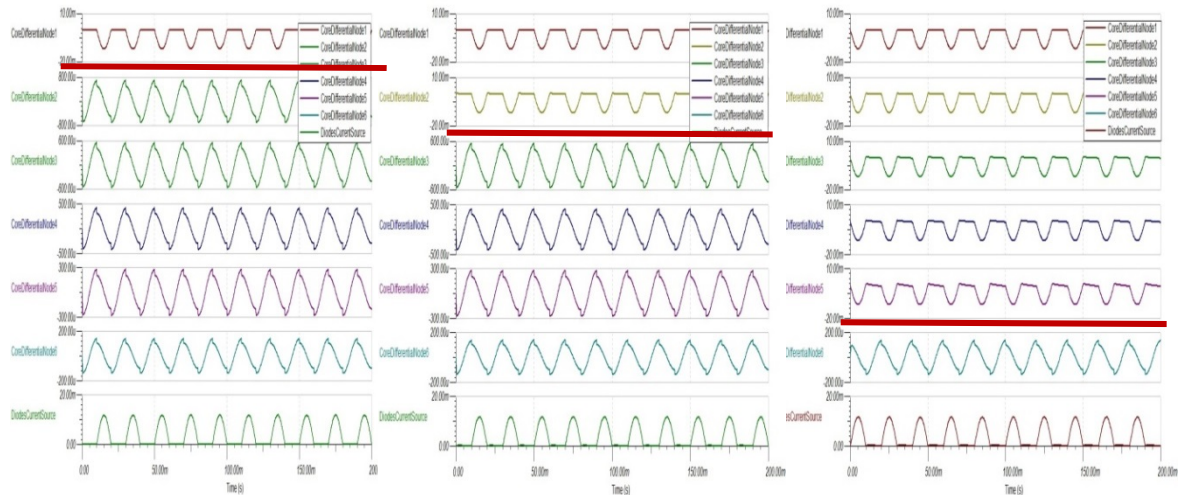


**Figure 6 Single Earth Fault Simulation**

A single earth fault (with 100 k leakage resistance) was placed in turn at nodes 1, 2 and 5, with only one fault at any one time. The simulation results were gathered together in Figure 6 above. All cable sections prior to the location of the fault have a distinctive rectified current difference pattern with the amplitude representing the leakage current (mA-level). Since the diode setup will not affect any sections after the fault, the current differences measured do not have the DC offset and will be very small ( $\mu$ A-level).

#### 4.3. Multiple Earth Faults

##### Single Conductor

It is also possible to have multiple recognisable earth faults simultaneously on one conductor. Current sensors installed before the first fault will receive the maximum difference that matches the reading from the grounding resistor. There will be an amplitude drop once the sensor passes an earth fault with the drop value itself being the earth leakage from the passed location. Until the sensor reaches the last fault location, the rectified signal remains, see Figure 7.



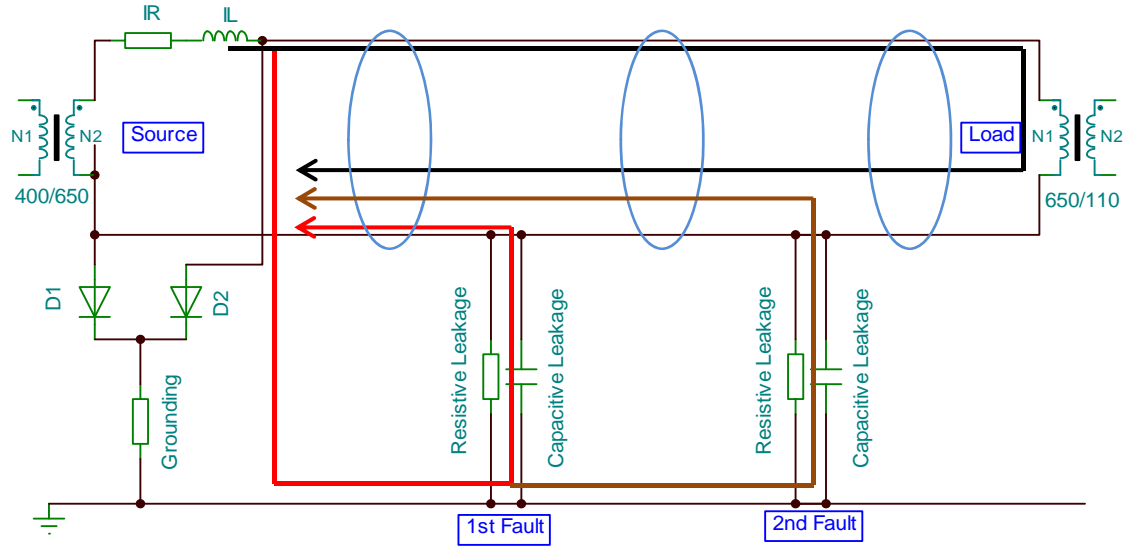


**Figure 7 Multiple Earth Faults**

Earth faults were put at nodes 2 and 5 (at 20 kiloOhm and 100 kiloOhm respectively). Figure 8 shows that the current difference before node 2 (where the first fault is located) has a rectified current pattern and its amplitude (15 mA) matches the reading from the grounding resistor. As for the current difference picked up within the cable sections between the two faults, it still has the rectified pattern but the amplitude (5 mA) is much smaller since the first earth fault current is no longer contributing. Once it passes the second fault, the rectified pattern disappears.

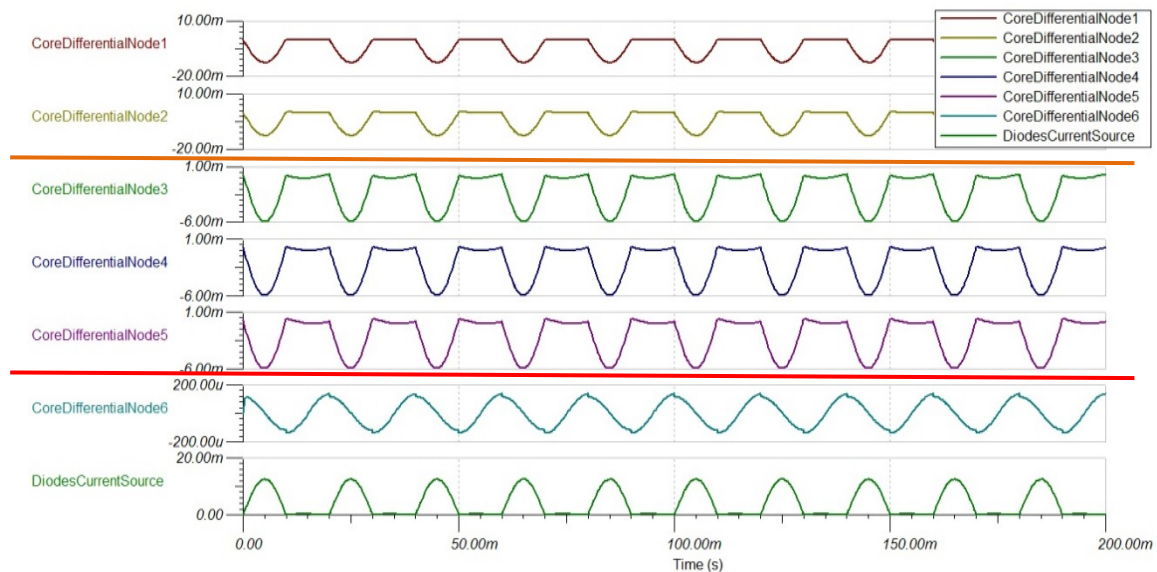


**Figure 8 Multiple Earth Fault Simulation**

### Both Conductors

Low resistance earth faults on both conductors, resulting in a major short circuit in the system, are very unlikely to happen since the first earth fault is usually detected immediately and will be cleared before the development of a second fault. However, high resistance earth leakage from both conductors is possible and can be a potential danger to the network. The simulation result is discussed below.

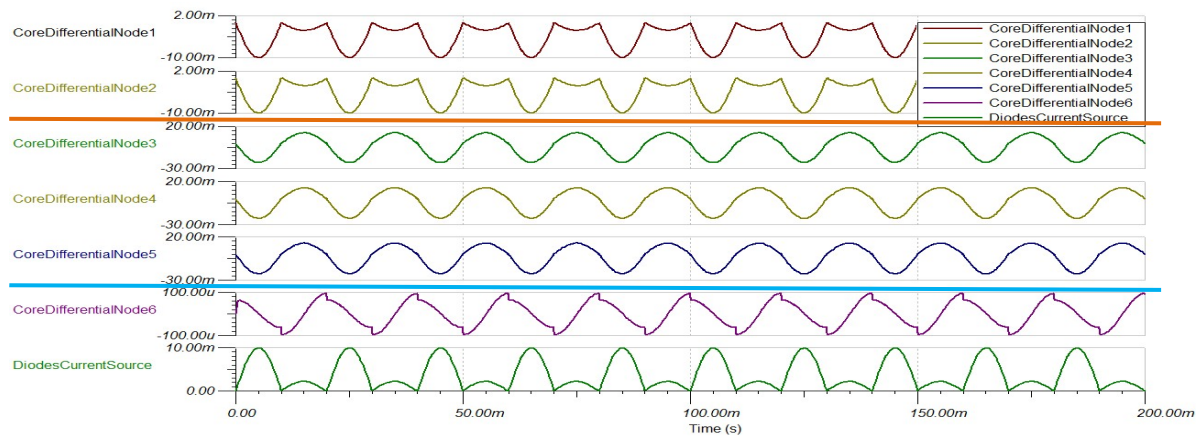


**Figure 9 Earth Faults on Both Conductors**

Similar to the previous setup, earth faults were put at nodes 2 and 5 (20 kilo Ohm and 100 kilo Ohm respectively) but on the different conductors. As shown in Figure 9 above, before the first fault, the current difference still has a rectified pattern and the grounding resistor reading indicates that both conductors are leaking. The sections between the two faults have current differences similar to the grounding resistor reading but alternating in both directions since there is leakage from both conductors. The pattern disappears where the sensor passes the last fault.

## 5. Lab Experiments

### 5.1. Current Difference Measurement

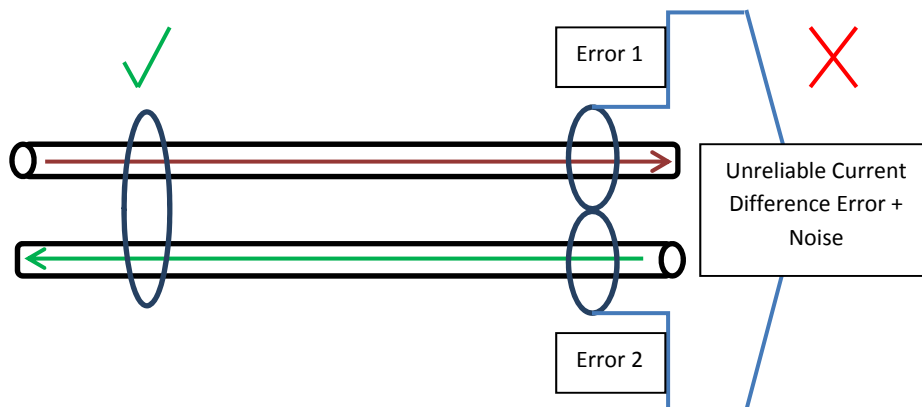


**Figure 10 Current Difference Measurement**

The out and return currents should be identical, but in opposite directions, feeding the loads. The difference between the out and return currents in a cable can, in principle, be determined by measuring the current of the out and return conductors independently and computing the difference. However, the difference is usually very small compared to the load current that flows through the cable. Taking into consideration the accuracy of individual current sensors, precision errors and computational errors, it is unlikely that the difference will be usable. Although pre-calibration of the sensor can minimise error, auto-calibration is still needed for any temperature-sensitive sensor so that the readings will have a consistent accuracy.

Consider the current observed by clamping a current sensor around the whole cable (common mode current). A Hall Effect current sensor or Rogawski Coil should be able to measure the small current difference. There are two practical problems to consider. One is that a practical sensor does not measure exactly zero when the load current is large. The other is that there can be genuine common-mode currents flowing in both conductors that the sensor observes. The signal to noise ratio can be significantly improved by using phase locked loop correlation methods.



## 5.2. Experiment Setup

Two sets of railway signalling B2 aluminium cable on cable drums were connected together with one end connected to a floating power supply and the other end connected with a variable power resistor. The rectifier setup was located at the source side with a high resistance variable resistor connected to a third conductor that was used to represent the earth. A high resistance earth fault was deliberately put at the exposed conductors where cable from one drum joined to the cable of the second drum. 16-bit NI-PXI was used for data acquisition. The source voltage level used for lab verification was 30 V at 50 Hz and all the other parameters were set up proportionally smaller in order to maintain the right leakage/load current ratio. Several current sensors were deployed along the cable to pick up the current difference from multiple locations. A bandpass filter was applied to filter out high frequency harmonics and noise and PLL was used to lock into the 100 Hz fundamental. Filtering and correlation were done in software for lab verification. The system flow chart and test parameters are shown below.

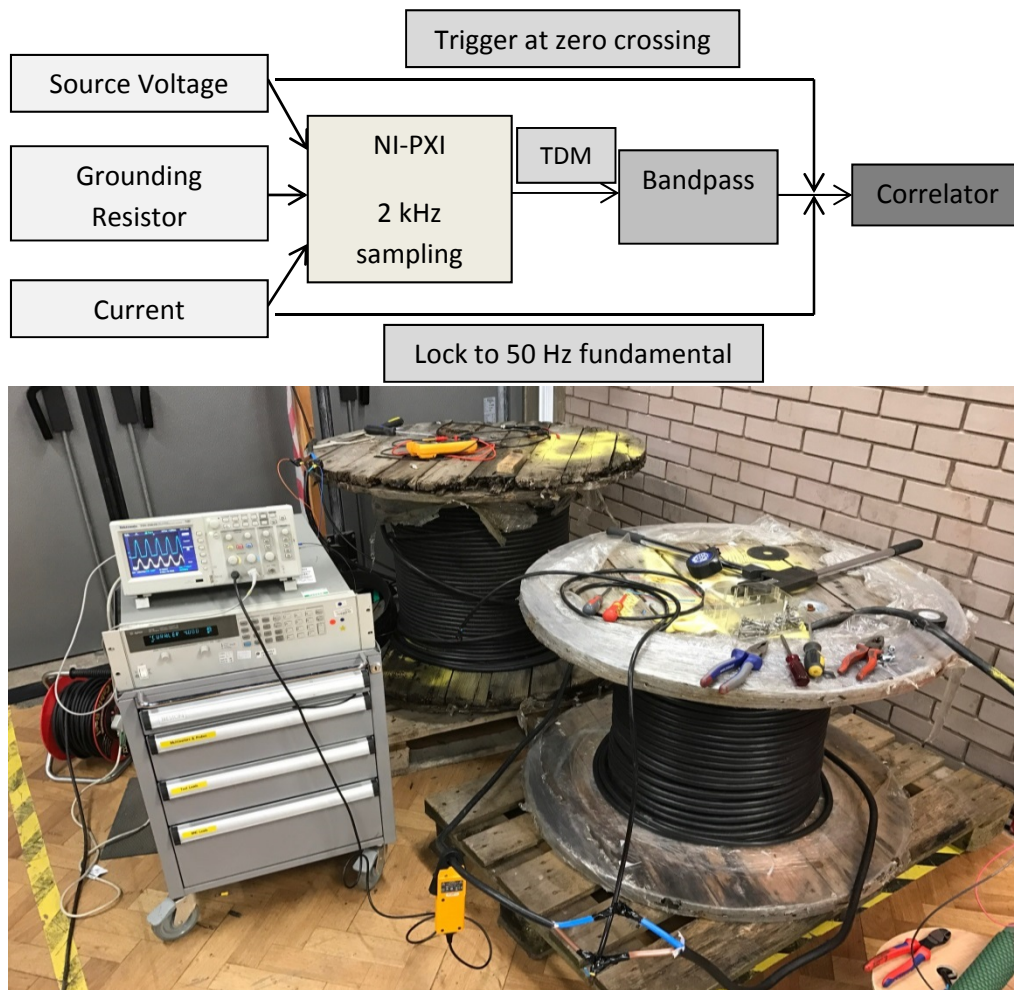


Figure 11 Experiment Setup

## 6. Test Results

Parameters	650 V AC Signalling Power	Lab Testing Environment
Length	10 km	100 m
Voltage Level	650 V 50 Hz	30 V 50 Hz
Grounding Resistance	0 – 100 k $\Omega$	0 – 5 k $\Omega$
Leakage Resistance	10 – 300 k $\Omega$	3 – 15 k $\Omega$
Leakage Current	10 – 65 mA	2 - 10 mA

<b>Load Current</b>	3 – 12 A	0.35 – 0.7 A
<b>Current Sensor Used</b>	Fluke i30, MAGNELAB SCT-0400-005 CWT, Power Electronic Measurements Ltd	

**Figure 12 Parameters in Lab Environment**

The source end grounding resistor will always have a clean voltage waveform without any post-processing as long as the earth fault is big enough to activate the diodes. The challenging part is to get a recognisable current difference. If the leakage current is large enough (tens of mA), the difference current pattern can be seen on an oscilloscope directly.

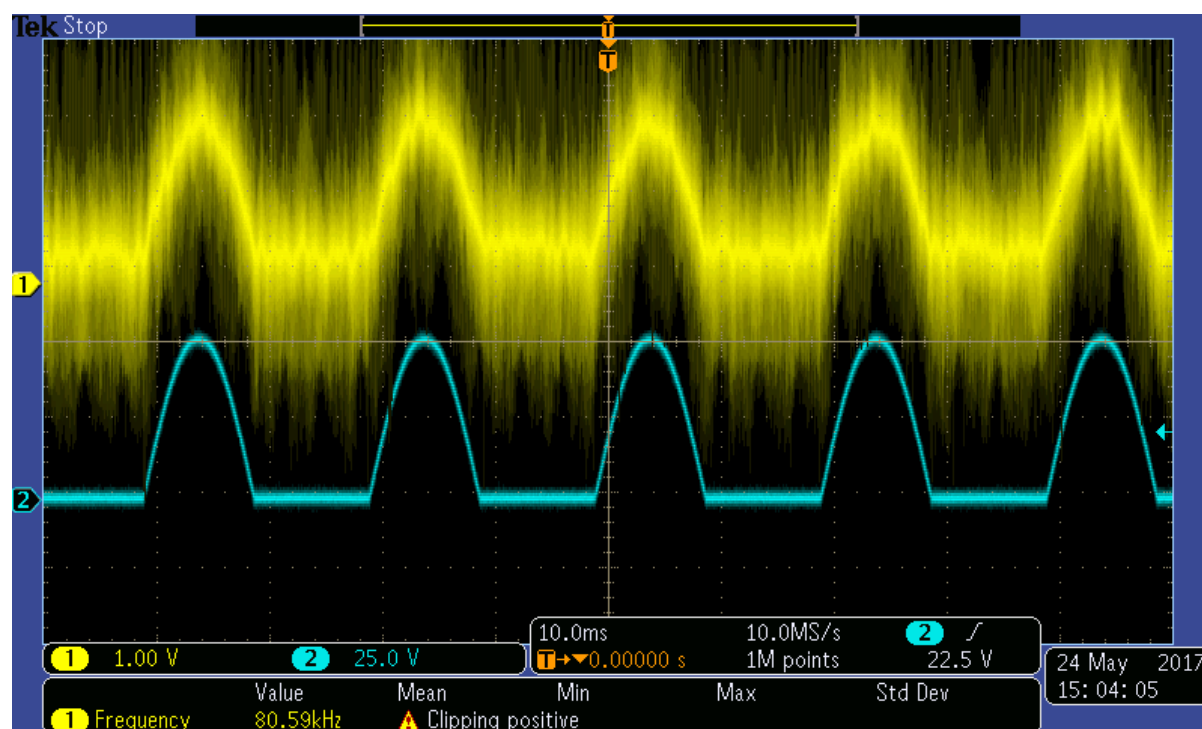


**Figure 13 Differential Current on the Oscilloscope**

In Figure 13, channel 2 (blue) is the voltage across a known grounding resistor and channel 1 (yellow) is the differential current picked up at a random location along the cable. Despite there being significant noise in the current difference waveform, the curve aligns with the rectified voltage pattern in channel 1, which indicates that it was picked up before the earth fault location. 3 different current sensors were used in the test and the results were very similar, which means the type of the current sensor is not essential in this case, since it is the pattern that matters rather than the exact magnitude in this case.

However, in most cases,  $I_D$  (current difference) is rather small because of a relatively higher leakage resistance, making it very difficult to recognize the rectified pattern directly without post-processing.

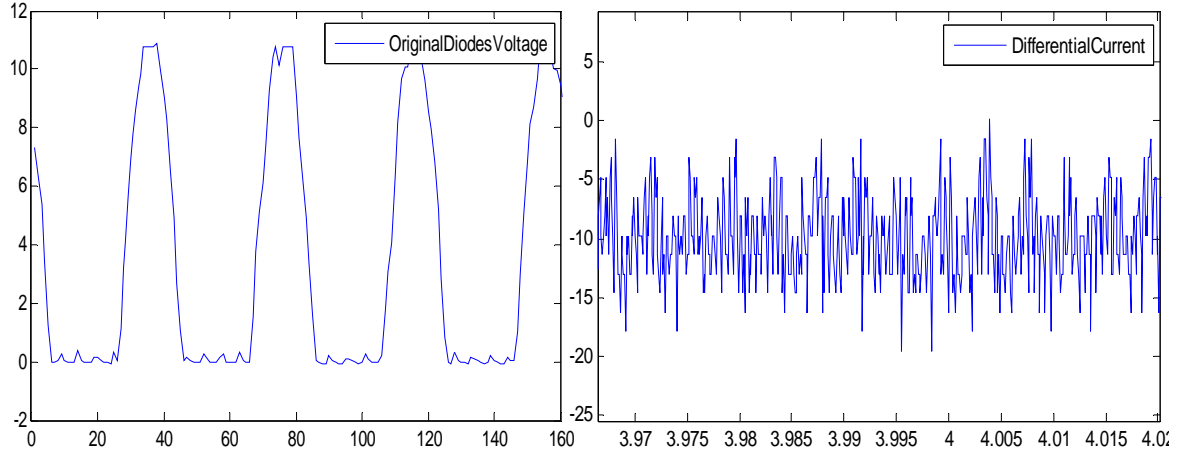


**Figure 14 High Resistance Current Difference**

The grounding resistor reading, shown in Figure 14, suggests that one of the conductors has a noticeable amount of earth leakage current but the differential current reading is too noisy to be interpreted by eye. Thus, phase locked loop based correlation is needed in order to reveal the distinctive periodic pattern. The results after correlation are shown below in Figure 15.

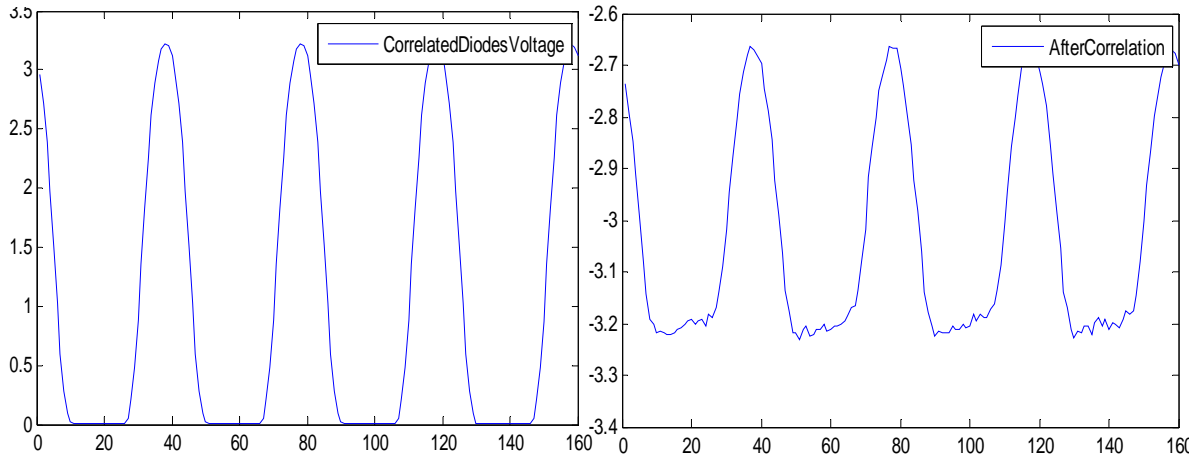


**Figure 15 High Resistance Current Difference Correlation (6 minutes of data)**

The total correlation process is given as:

$$C_{DN}(k) = \sum_{i=1}^{N_c} I_{DN(i)}(k)$$

Where  $N_c$  is the total number of cycles and  $K$  is the sample index within each cycle.

Total current difference consists of pure current difference and noise, thus the measurement samples can be represented as:

$$I_{DN}(k) = I_D(k) + I_N(k)$$

Total correlation is represented by:

$$C_{DN}(k) = C_D(k) + C_N(k) = \frac{1}{N_c} \sum_{i=1}^{N_c} I_{D(i)}(k) + \frac{1}{N_c} \sum_{i=1}^{N_c} I_{N(i)}(k)$$

Further approximation can be done since the current difference  $I_D$  is periodic:

$$C_{DN}(k) = I_{D(i)}(k) + \frac{1}{N_c} \sum_{i=1}^{N_c} I_{N(i)}(k)$$

Considering the non-periodic noise current  $I_N$  will not correlate with itself, the noise reduction with the progressive correlation cycle  $N_c$  is given by:

$$\lim_{N_c \rightarrow \infty} \frac{1}{N_c} \sum_{i=1}^{N_c} I_{N(i)}(k) \rightarrow 0 + \Phi$$

Even if the mean noise is zero, the total correlation can still have a possible DC-offset  $\Phi$ , which is the unbalanced error from the current sensor. However, it does not affect the locating procedure since the rectified current pattern will still appear on top of the DC-offset. Noise reduction is limited by the sampling resolution and the total number of cycles taken. The smaller the leakage, the longer the correlation is required (shown in Figure 16 below). This is limited by the resolution of the sampling ADC.

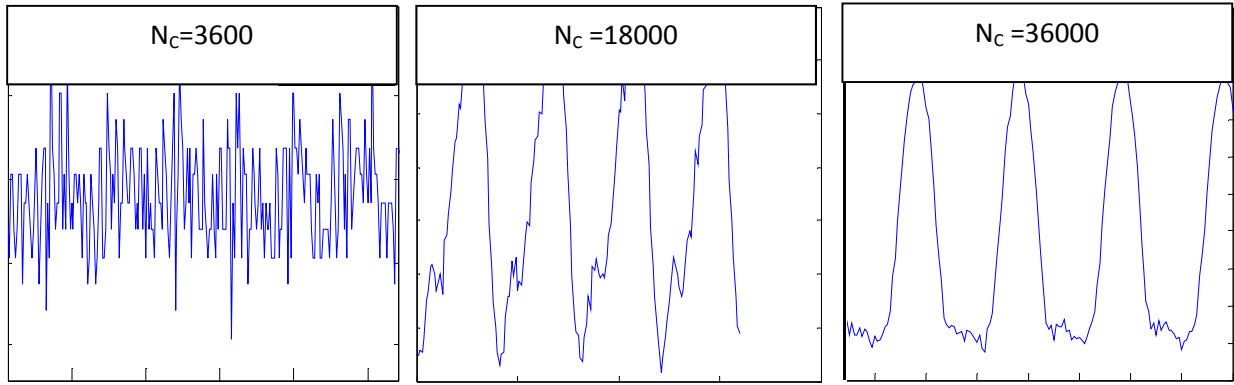


**Figure 16 Noise Reduction**

## 7. Suggested Monitoring System

A suggested insulation monitoring system for the 650 V signalling power supply is given below.

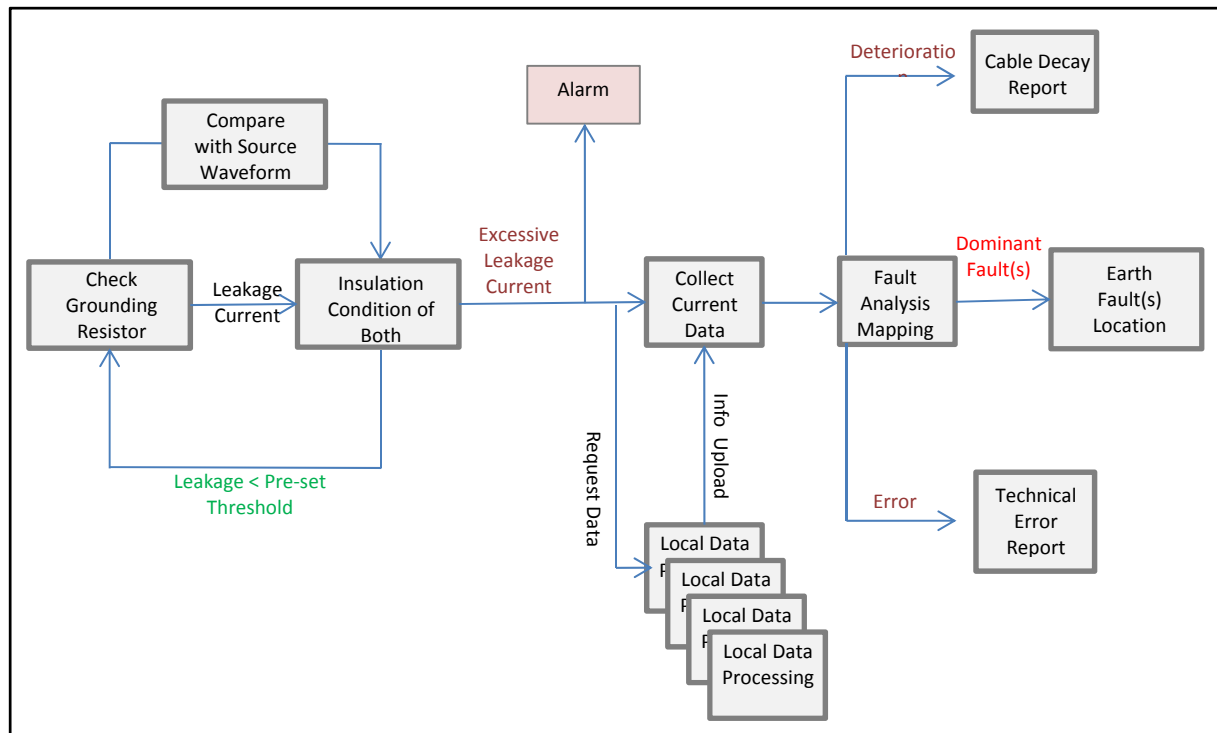


Figure 17 Suggested Insulation Monitoring System

### 7.1. Fault Location

The insulation condition of the network will be constantly calculated by monitoring the voltage across the source-side grounding resistor. All the distributed local current sensors will measure the current difference simultaneously and upload the correlation results to the cloud server constantly, whereas in a repeated signal injection based fault location process, a scheduled measuring process is required to make sure that only one node is connected to the network at a time.

Fault location analysis process will be triggered on the network/total IR(Insulation resistance). Multiple level of IR threshold will be set in accordance to the network maintenance protocol. Once the network IR drops below a threshold of interest, corresponding alarm will be raised. All the latest uploaded data from all the sensors will then be pulled and analysed in order to locate the dominant insulation fault(s). Results and all the detailed information will be send to the maintenance team afterwards so that scheduled maintenance can be carried out as soon as possible.

### 7.2. Data Trending

Apart from triggering the fault location analysis when the network IR drops below the fault threshold, all the measurement data stored in the cloud server shall be analysed on a weekly or even daily base for prognosis and data trending purpose. Reasonable deductions (e.g. which cable section that is most likely to fail, how long will it take for the network IR to drop below the threshold, etc.) shall be made and will be taken into consideration during the fault location process discussed before. This is particularly useful in situations where no dominant fault presents (e.g. general cable decay and degradation).

## 8. Summary

A potential condition monitoring method for railway signalling power systems based on current difference analysis is introduced in this paper. Simulation results show that the proposed method is able to identify and locate high resistance earth faults. Initial lab test results have been encouraging. Earth leakage can be detected as long as the fault is significantly larger than the diode reverse leakage current. The resolution of the proposed distributed fault locating scheme will be limited by its total number of sensors deployed along the network, but the suggested server-based data analysis will make the cost per monitoring point much lower than other technologies.

## References

- [1] S. Hua, "RAILWAY SIGNALLING POWER – ECONOMIC AND PERFORMANCE ENHANCEMENTS FOR TOMORROW'S RAILWAY," Network Rail2011.
- [2] "IEEE Guide for Fault Locating Techniques on Shielded Power Cable Systems," *IEEE Std 1243-1997*, pp. 1-34, 2007.
- [3] K. Gi-Taek, K. Hyuck-Soo, and C. Hmg-Yong, "Wavelet transform based power transmission line fault location using GPS for accurate time synchronization," in *Industrial Electronics Society, 2001. IECON '01. The 27th Annual Conference of the IEEE*, 2001, pp. 495-499 vol.1.
- [4] S. Nath, A. Chakrabarti, and A. K. Mukhopadhyay, "A microcomputer-based unique digital fault diagnosis scheme of radial transformer feeders," *Power Delivery, IEEE Transactions on*, vol. 21, pp. 1824-1829, 2006.
- [5] K. Srinivasan and A. St.-Jacques, "A new fault location algorithm for radial transmission lines with loads," *Power Delivery, IEEE Transactions on*, vol. 4, pp. 1676-1682, 1989.
- [6] S. Santoso, R. C. Dugan, J. Lamoree, and A. Sundaram, "Distance estimation technique for single line-to-ground faults in a radial distribution system," in *Power Engineering Society Winter Meeting, 2000. IEEE*, 2000, pp. 2551-2555 vol.4.
- [7] A. A. Girgis, C. M. Fallon, and D. L. Lubkeman, "A fault location technique for rural distribution feeders," *Industry Applications, IEEE Transactions on*, vol. 29, pp. 1170-1175, 1993.
- [8] S. M. Brahma and A. A. Girgis, "Fault location on a transmission line using synchronized Voltage measurements," *Power Delivery, IEEE Transactions on*, vol. 19, pp. 1619-1622, 2004.
- [9] G. Preston, Radojevic, x, Z. M., C. H. Kim, and V. Terzija, "New settings-free fault location algorithm based on synchronised sampling," *Generation, Transmission & Distribution, IET*, vol. 5, pp. 376-383, 2011.
- [10] T. C. Henneberger and P. G. Edwards, "Bridge methods for locating resistance faults on cable wires," *Bell System Technical Journal, The*, vol. 10, pp. 382-407, 1931.
- [11] Y.-x. Liao, K. Zhou, Y.-x. Su, and K. Qi, "Pre-location Approach for 10kV High Resistance Cable Fault Based on Improved Bridge Method," in *High Voltage Engineering and Application, 2008. ICHVE 2008. International Conference on*, 2008, pp. 359-361.
- [12] H. Amira, M. Hfaiedh, and M. Valentin, "Quasi-balanced bridge method for the measurements of the impedances," *Science, Measurement & Technology, IET*, vol. 3, pp. 403-409, 2009.
- [13] M. Gilany, D. K. Ibrahim, and E. S. T. Eldin, "Traveling-Wave-Based Fault-Location Scheme for Multiend-Aged Underground Cable System," *Power Delivery, IEEE Transactions on*, vol. 22, pp. 82-89, 2007.
- [14] J. Chae-kyun and L. Jong-beom, "Fault location algorithm on underground power cable systems using noise cancellation technique," in *Transmission and Distribution Conference and Exposition, 2008. T&D 2008. IEEE/PES*, 2008, pp. 1-7.
- [15] M. Paolone, A. Borghetti, and C. A. Nucci, "An automatic system to locate phase-to-ground faults in medium voltage cable networks based on the wavelet analysis of high-frequency signals," in *PowerTech, 2011 IEEE Trondheim*, 2011, pp. 1-7.
- [16] P. Chen and K. Wang, "Fault location technology for high-voltage overhead lines combined with underground power cables based on travelling wave principle," in *Advanced Power System Automation and Protection (APAP), 2011 International Conference on*, 2011, pp. 748-751.
- [17] H. Li, "Study on the fault detection of railway signaling cable based on wavelet and virtual instrument," in *Communication Software and Networks (ICCSN), 2011 IEEE 3rd International Conference on*, 2011, pp. 476-479.
- [18] N. H. Rahim, I. Sutan Chairul, S. Ab Ghani, M. S. Ahmad Khair, N. Abas, and Y. H. Md Thayoob, "Simulation of TDR circuit for the analysis of wave propagation in XLPE cable model," in *Power and Energy (PECon), 2012 IEEE International Conference on*, 2012, pp. 796-801.



- [19] M. Da Silva, M. Oleskovicz, and D. V. Coury, "A Fault Locator for Three-Terminal Lines Based on Wavelet Transform Applied to Synchronized Current and Voltage Signals," in *Transmission & Distribution Conference and Exposition: Latin America, 2006. TDC '06. IEEE/PES*, 2006, pp. 1-6.
- [20] "IEEE Guide for Determining Fault Location on AC Transmission and Distribution Lines," *IEEE Std C37.114-2014 (Revision of IEEE Std C37.114-2004)*, pp. 1-76, 2015.
- [21] C. F. Jensen, O. M. K. K. Nanayakkara, A. D. Rajapakse, U. S. Gudmundsdottir, and C. L. Bak, "Online fault location on AC cables in underground transmission systems using sheath currents," *Electric Power Systems Research*, vol. 115, pp. 74-79, 10// 2014.
- [22] R. A. Guinee, "A novel pseudonoise tester for transmission line fault location and identification using pseudorandom binary sequences," in *Defect and Fault Tolerance in VLSI and Nanotechnology Systems (DFT), 2012 IEEE International Symposium on*, 2012, pp. 225-232.
- [23] J. Wang, P. E. C. Stone, Y.-J. Shin, and R. A. Dougal. (2010, Application of joint time–frequency domain reflectometry for electric power cable diagnostics. *IET Signal Processing* 4(4), 395-405. Available: <http://digital-library.theiet.org/content/journals/10.1049/iet-spr.2009.0137>
- [24] C. Furse, P. Smith, M. Safavi, and L. Chet, "Feasibility of spread spectrum sensors for location of arcs on live wires," *Sensors Journal, IEEE*, vol. 5, pp. 1445-1450, 2005.
- [25] L. A. Griffiths, R. Parakh, C. Furse, and B. Baker, "The invisible fray: a critical analysis of the use of reflectometry for fray location," *Sensors Journal, IEEE*, vol. 6, pp. 697-706, 2006.